Structural basis of ClpXP recognition and unfolding of ssrA-tagged C-degron substrates

Xue Fei[1,*], Tristan A. Bell[1,*], Sarah R. Barkow[2],

Tania A. Baker[1], and Robert T. Sauer[1]

Departments of Biology[1] and Chemistry[2]

Massachusetts Institute of Technology

Cambridge, MA, USA 02139

[*] These authors contributed equally to this work

Corresponding author: R.T Sauer; bobsauer@mit.edu

Running title: *ClpXP-substrate recognition*

Key words: AAA+ protease; degron; cryo-EM structures; tmRNA tagging; degradation specificity; recognition complex; intermediate complex

All cells degrade partially synthesized proteins when ribosomes fail to complete normal translation[1]. In Escherichia coli and other eubacteria, the tmRNA system rescues stalled ribosomes and cotranslationally adds an ssrA tag to the C-terminus of the incomplete protein to direct degradation by ClpXP and other AAA+ proteases, thereby safeguarding proteome integrity[2]. Here, we present two cryo-EM structures of ClpXP bound to the ssrA degron, which explain initial degron recognition and subsequent movement into the motor's central channel. Our studies illuminate how ClpXP unfolds substrates with degrons of different lengths and transitions from specific recognition into a nonspecific unfolding and translocation machine. Many AAA+ proteases and protein-remodeling motors likely employ similar strategies.

ClpXP and related AAA+ proteases maintain cellular health by degrading incomplete, damaged, or unneeded proteins in a multistep process that must be specific to avoid destruction of essential intracellular proteins[3]. In bacteria and eukaryotic organelles, AAA+ proteases typically recognize substrates via short N- or C-terminal peptide sequences. *E. coli* ClpXP, for example, degrades proteins bearing a C-terminal AANDENYALAA-COO^- degron called the ssrA tag that is added during tmRNA-rescue of stalled ribosomes[2]. AA-COO^- is the most important element of this degron for ClpXP degradation[4], and related degrons terminating in this dipeptide target other cellular proteins to ClpXP[5-7]. The ssrA tag initially binds in the axial channel of the hexameric AAA+ ClpX ring, where the pore-1, pore-2, and RKH loops play critical roles in recognition[8-11]. Subsequent mechanical reactions requiring ATP hydrolysis unfold

adjacent regions of native protein structure and then translocate the denatured polypeptide through the channel and into the degradation chamber of the double-ring $ClpP_{14}$ peptidase for proteolysis[12]. Here, we establish the molecular basis of the recognition step in targeted ClpXP degradation of ssrA-tagged proteins. We also characterize subsequent unfolding/translocation steps that initiate processive degradation (Fig. 1A).

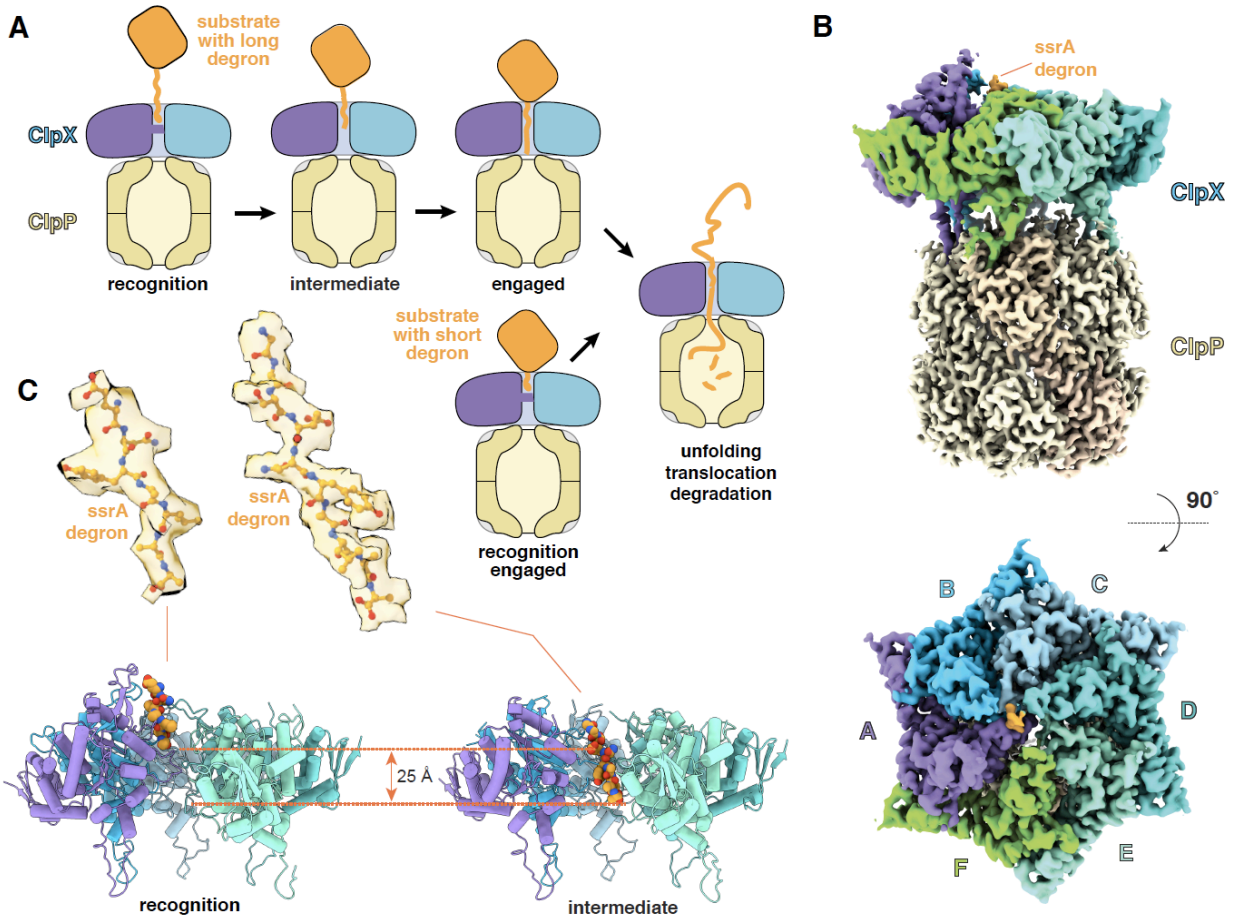

Figure 1. ClpXP complexes with ssrA degrons. (A) Models for recognition and engagement of substrates with long (~20 residue) or short (~5 residue) degrons. In all figures, ClpX is colored blue, green, or purple; ClpP is yellow/gold; and substrate is orange. (B) Side and top views of density from the recognition complex. (C) The upper portion of the panel shows transparent density for the ssrA degron (stick representation) in the recognition and intermediate complexes; the lower portion shows the offset positions of the ssrA degron (space-filling representation) in the channel of ClpX (cartoon representation) in both complexes after removal of subunit F.

For cryo-EM, we used an ssrA-tagged green fluorescent protein substrate (GFP-G_3YG_9SENYALAA; ssrA residues underlined), a single-chain *E. coli* ClpX$^{\Delta N}$ pseudohexamer[13,14], and *E. coli* ClpP. Approximately 15 s before vitrification, we combined the GFP substrate and ATP with a mixture of the ClpX$^{\Delta N}$ variant, ClpP$_{14}$, and ATPγS. From this single experiment, classification and three-dimensional reconstruction of EM images containing one ClpX$^{\Delta N}$ pseudohexamer and one ClpP tetradecamer generated density maps of ClpX bound to one heptameric ring of ClpP$_{14}$ and 7-10 residues of the ssrA degron in two distinct conformations (Figs. 1B, 1C; Table 1). As seen previously[14,15], subunits of the ClpX$^{\Delta N}$ hexamer formed a shallow spiral (labeled ABCDEF top to bottom), which docked asymmetrically with a flat ClpP$_7$ ring. The pore of the cis ClpP ring contacting ClpX was open, as expected[14,15], but the pore of the trans ClpP ring was closed in both new structures. The ssrA degron bound in the top of the ClpX channel in a structure we call the recognition complex and moved ~25 Å or 6 residues deeper into the channel in a structure we call the intermediate complex (Fig. 1C).

In the recognition complex, the ssrA degron bound high in the ClpX channel and access to the lower channel was blocked by a previously unvisualized conformation of the pore-2 loop of ClpX subunit A (Figs. 1C, 2A, 2B). T199 and V202 side chains from this pore-2 loop contacted the Cβ methyl and α-COO$^-$ of the C-terminal alanine of the ssrA degron. Y153 and V154 side-chain or main-chain groups from pore-1 loops (subunits A/B) or R228 and H230 side chains from RKH loops (subunits B/C/D/F) made additional

contacts with the AA-COO⁻ or neighboring degron regions (Figs. 2A, 2B, 2C; movie S1). Multiple experiments support the role of this structure in specific substrate recognition.

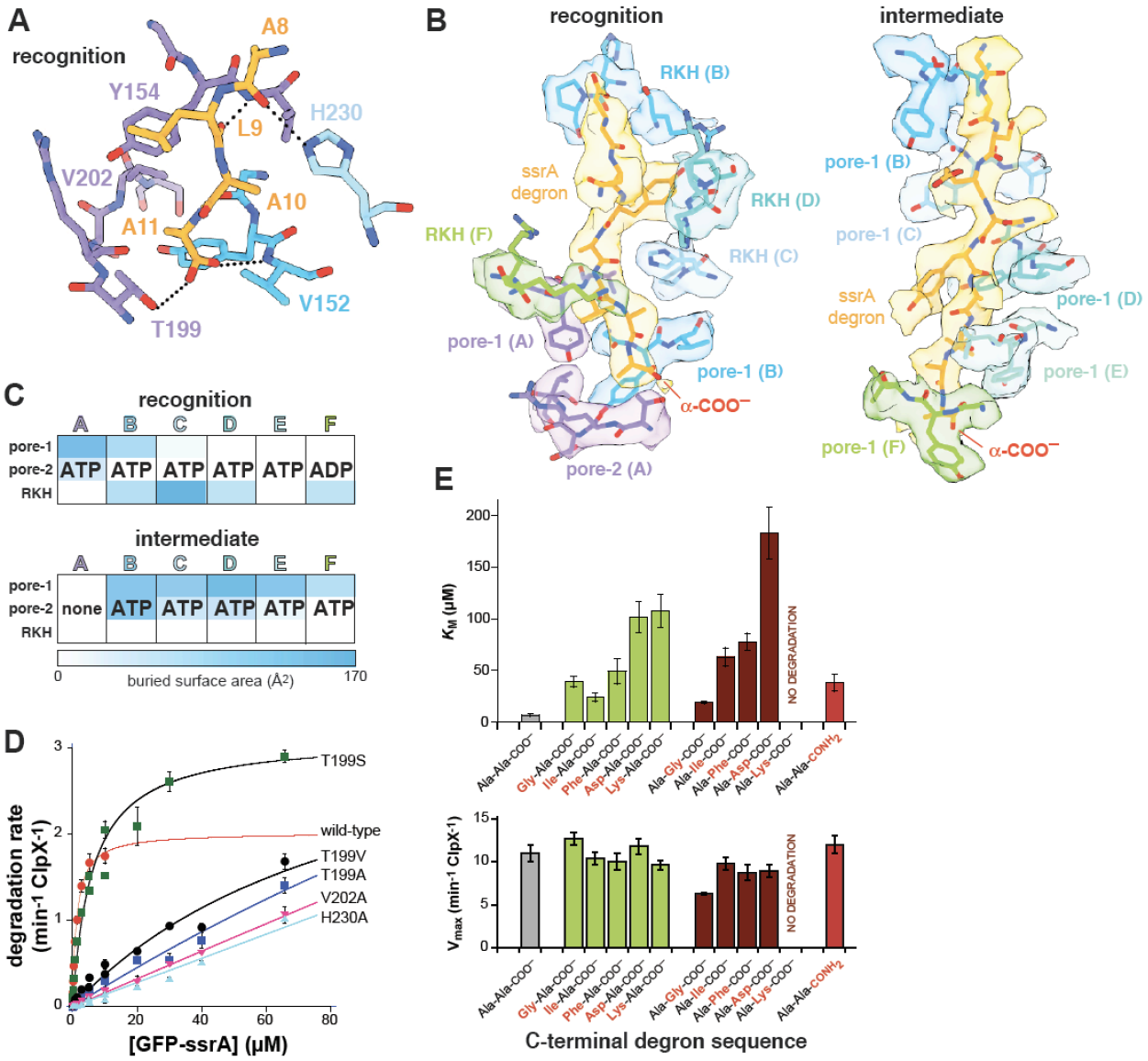

Figure 2. ClpX-degron interactions. (A) Key ClpX residues (blue or purple) and the C-terminal segment of the ssrA degron (gold) in the recognition complex are shown in stick representation. Dashed lines indicate hydrogen bonds. (B) ClpX-degron contacts in the recognition and intermediate complexes. ClpX or degron residues are shown in stick representation with semi-transparent density. (C) Subunit nucleotide state and degron/pore-loop interactions in the recognition and intermediate complexes. (D) Degradation of GFP-ssrA by $ClpX^{\Delta N}$/ClpP and variants. Data are means ± SD (n = 3 to 6), and lines are fits to the Michaelis-Menten equation. Fitted K_M values (μM) were 1.3 ± 0.2 (wild type), 6.3 ± 1.7 (T199S), and 89 ± 34 μM (T199V). Fitted V_{max} values (min^{-1} $ClpX^{-1}$) were 2.0 ± 0.1 (wild type), 3.1 ± 0.2 (T199S), and 3.7 ± 2.0 (T199V). For the T199A, V202A, and H230A variants, unconstrained fits had huge error limits, and fits with V_{max} constrained to ≥ 4 min^{-1} $ClpX^{-1}$ gave K_M values from 140 to 240 μM. (E) Steady-state K_M (top) and V_{max} (bottom) parameters (means ± SD; n = 3) for ClpXP degradation of synthetic peptide substrates containing an aminobenzoic-acid (ABZ) fluorophore and nitrotyrosine (Y^{NO2}) quencher

(wild-type sequence ABZ-FAPHMALVPY^{NO2}GYGGKKLAANDENYALAA; gray bar) with substitutions for the penultimate residue (green bars), C-terminal residue (dark red bars), or α-carboxylate (red bar).

First, previously characterized Y153A, V154F, and R228A ClpX mutations increase K_M for ClpP degradation of ssrA-tagged substrates 50-fold or more[8-11], as did newly constructed T199A, T199V, V202A, and H230A mutations (Fig. 2D). By contrast, K_M for degradation by the conservative T199S variant increased only ~4-fold (Fig. 2D), supporting a key role for a hydrogen bond between the side-chain hydroxyl of T199 and degron α-carboxylate (Fig. 2A). Second, compared to the wild-type enzyme, R228A ClpXP displayed increased specificity against an N-degron substrate[9]. Third, human ClpXP has leucines at positions corresponding to T199 and H230 in *E. coli* ClpX and does not degrade ssrA-tagged substrates, but a human hybrid containing the pore-2 and RKH loops of the *E. coli* enzyme acquires this activity[10]. Finally, in 29-residue peptide substrates, we found that mutation of the penultimate or C-terminal ssrA residues increased K_M for ClpXP degradation but had little effect on V_{max} (Fig. 2E). Mutation of the antepenultimate leucine of the ssrA tag or tyrosine two residues upstream also increases K_M modestly[6], which can be rationalized based upon recognition-complex contacts.

In the intermediate complex, five ClpX pore-1 loops and four pore-2 loops packed against degron side chains with a two-residue periodicity (Figs. 2B, 2C, movie S2) observed previously in ClpXP complexes with other substrates and in different AAA+ proteases and protein-remodeling machines[14-16]. These enzyme structures are thought to reflect snapshots during non-specific translocation. Indeed, ClpXP translocates a variety of sequences, including polymeric tracts of glycine, proline, lysine, arginine,

glutamate, and glutamine[17], and specific contacts observed in the recognition complex were absent in the intermediate complex. Non-specific translocation allows ClpXP to degrade any protein after degron recognition and unfolding of attached native structure. Prior to recognition, our results suggest that the ClpX channel is occluded, thereby preventing non-specific binding and degron-independent degradation.

Can a stable protein substrate be unfolded directly from the recognition complex or must a degron move deeper into the ClpX channel, with concomitant engagement of additional pore-1 and pore-2 loops, to allow mechanical substrate denaturation? The 20-residue degron of GFP-G_3YG_9SENYALAA could move from its position in the recognition complex deeper into the channel without GFP unfolding, and thus our structures don't answer this question. However, if direct unfolding from the recognition complex is possible, then a degron of ~5 residues should be sufficient for degradation. Hence, we constructed substrates with degrons of 3, 5, 7, 9, or 11 residues following the last structured residue of GFP (Fig. 3A) and assayed degradation. Strikingly, GFP-LAA was not degraded, whereas GFP-YALAA and substrates with longer tags were robustly degraded (Fig. 3B). Modeling revealed that the native barrel of GFP-YALAA docked snugly with the top of the AAA+ ClpX ring, with the YALAA in the same position as in the recognition complex (Figs. 3C, 3D; movie S3). By contrast, the tag of GFP-LAA was too short to allow formation of recognition-complex contacts without severe steric clashes with ClpX. It might be argued that the C-terminal β-strand of GFP-YALAA, which is ~20 residues in length, unfolds to allow additional C-terminal residues of the substrate to bind deeper in the channel of ClpX. However, global GFP unfolding occurs with a half-life of years and the C-terminal β-strand remains stably associated even when it is

non-covalently attached to the remaining native structure[18,19]. The inability of ClpXP to degrade GFP-LAA is also inconsistent with a model in which the C-terminal β-strand of GFP denatures. We conclude that a power stroke initiated directly from the recognition complex can unfold GFP-YALAA and similar short-degron substrates (Fig. 3E).

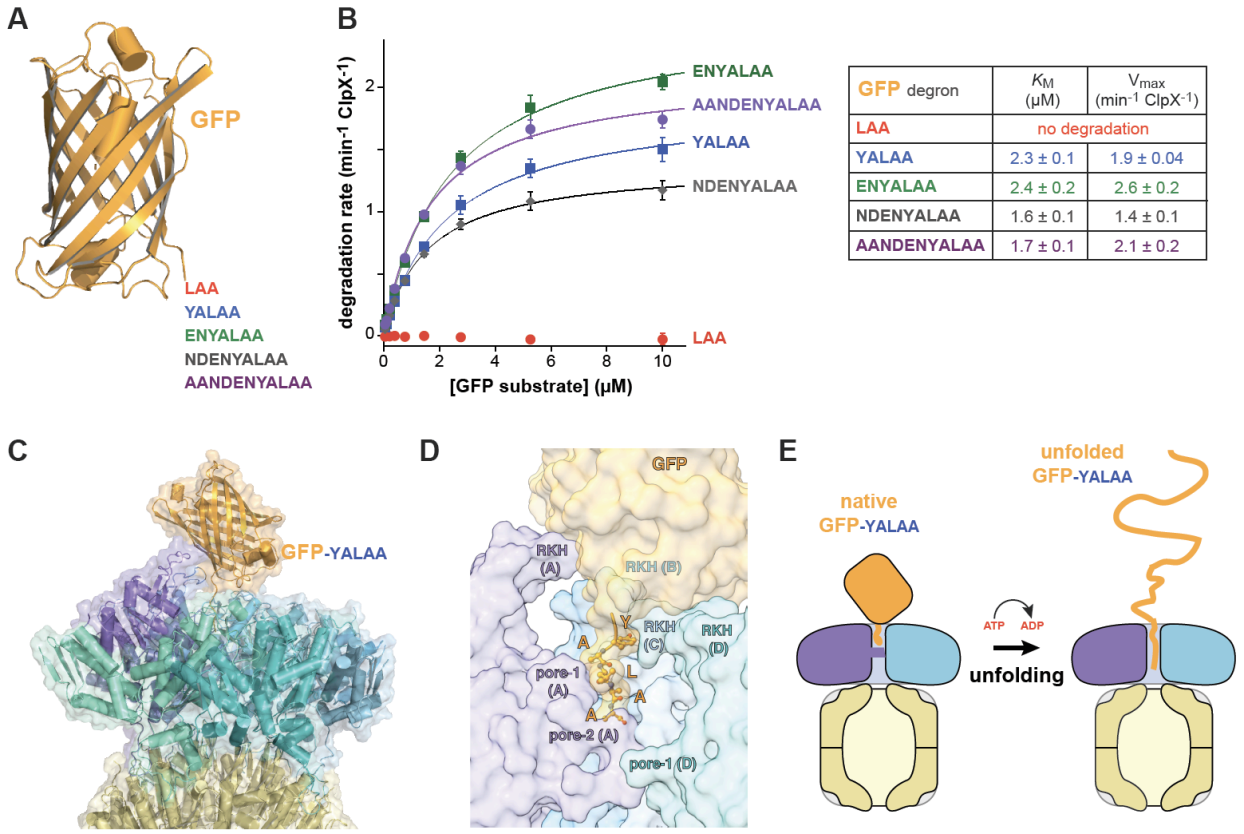

GFP degron	K_M (μM)	V_{max} (min^{-1} ClpX^{-1})
LAA	no degradation	
YALAA	2.3 ± 0.1	1.9 ± 0.04
ENYALAA	2.4 ± 0.2	2.6 ± 0.2
NDENYALAA	1.6 ± 0.1	1.4 ± 0.1
AANDENYALAA	1.7 ± 0.1	2.1 ± 0.2

Figure 3. Degradation dependence on degron length. (A) Cartoon of GFP (pdb 1EMA[24]) with degron tails of 3, 5, 7, 9, and 11 residues. (B) Plots of steady-state ClpX$^{\Delta N}$/ClpP degradation rates (means ± SD; n=3) as a function of substrate concentration. Lines are fits to the Michaelis-Menten equation. Fitted K_M and V_{max} values represent averages of three independent determinations ± SD. (C) Model of GFP-YALAA bound to ClpXP (cartoon and semi-transparent surface representation) created by aligning the YALAA of GFP to the same sequence in the recognition complex and then minimizing clashes both manually and computationally. (D) Close-up view of the ClpX-GFP-YALAA model (subunits E and F removed) with the YALAA shown in ball-and-stick representation. (E) Cartoon in which one power stroke unfolds GFP by translocating the YALAA degron six residues deeper into the channel of ClpX.

In the recognition complex, subunits ABCDE of ClpX contained ATP/ATPγS and subunit F contained ADP. In the intermediate complex, however, subunit A was nucleotide free

and the remaining subunits were ATP/ATPγS bound (Fig. 2C). Thus, it is plausible that ATP hydrolysis in subunit A of the recognition complex drives an unfolding power stroke and conversion to the intermediate complex. Movie S4 shows a morph illustrating the transition between these states. The 6-residue offset in the position of the ssrA tag between the two complexes (Fig. 1C) is consistent with optical-trap experiments that show a fundamental ClpXP translocation step of 5-8 amino acids[20,21]. Hence, for sufficiently short tags, a single recognition-complex power stroke could move the tag six residues deeper into the channel, unfolding native structure N-terminal to the tag in the process (Fig. 3E). For longer tags, including the 20-residue degron used for cryo-EM studies, continued translocation after the first power stroke would eventually bring the native protein in contact with the top of the ClpX channel, where additional power strokes could apply an unfolding force (Fig. 1A).

A recent study of the kinetics of ClpXP association with a substrate bearing a 20-residue ssrA degron provided evidence for three sequentially occupied substrate-bound conformations[22]. The first two are likely to correspond to our recognition and intermediate complexes. Conversion of the first to the second complex depended on the rate of ATP hydrolysis, as did formation of the third kinetically defined state, which is probably similar to the fully engaged complex depicted in Fig. 1A. Indeed, prior ClpXP complexes show the native portion of a protein substrate contacting the top of the central channel, with an attached peptide filling the channel[14]. Our results indicate that ClpX can unfold short-degron substrates directly from a closed-channel recognition complex and long-degron substrates from a subsequent open-channel engaged complex. Although unfolding in these two cases must be somewhat different, substrate

residues in the upper part of the channel are gripped most tightly during ClpXP unfolding of substrates with long degrons[23], supporting a model in which ClpX-substrate contacts near the top of the channel play key roles in both unfolding mechanisms.

The multistep mechanism proposed here for protein degradation by ClpXP is likely to be used by related AAA+ proteases that recognize unstructured degrons, as it nicely resolves how unfolding motors make initiation highly specific (and thus limited to appropriate protein targets) but then allow nonspecific unfolding and translocation for subsequent degradation. It is also reminiscent of transcription, translation, DNA replication, and protein secretion, which also require transitions from specific recognition conformations to complexes that utilize the chemical energy of ATP or GTP hydrolysis to processively and non-specifically move along their polymeric substrates.

ACKNOWLEDGMENTS

Supported by NIH grant GM-101988. We thank C. Xu, K. Song, and K. Lee at the Electron Microscopy Facility at the U. Mass. Medical School for advice and data collection.

AUTHOR CONTRIBUTIONS

X.F., T.A. Bell, S.R.B., and R.T.S. performed cryo-EM experiments, model building, or biochemical experiments. T.A. Baker and R.T.S. supervised research. All authors contributed to writing and/or revising the manuscript.

References

1. Buskirk, A.R. & Green, R. Ribosome pausing, arrest and rescue in bacteria and eukaryotes. *Philos. Trans. R. Soc. Lond. B Biol. Sci*. **372**,1716 (2017).

2. Keiler, K.C. Mechanisms of ribosome rescue in bacteria. *Nat. Rev. Microbiol.* **13**, 285–297 (2015).

3. Sauer, R.T. & Baker, T.A. AAA+ proteases: ATP-fueled machines of protein destruction. *Annu. Rev. Biochem*. **80**, 587–612 (2011).

4. Flynn, J.M., Neher, S.B., Kim, Y.I., Sauer, R.T. & Baker, T.A. Proteomic discovery of cellular substrates of the ClpXP protease reveals five classes of ClpX-recognition signals. *Mol. Cell* **11**, 671–683 (2003).

5. Neher, S.B., Villén, J., Oakes, E.C., Bakalarski, C.E., Sauer, R.T., Gygi, S.P. & Baker, T.A. Proteomic profiling of ClpXP substrates after DNA damage reveals extensive instability within SOS regulon. *Mol. Cell* **22**, 193–204 (2006).

6. Flynn, J.M., Levchenko, I., Seidel, M., Wickner, S.H., Sauer, R.T. & Baker, T.A. Overlapping recognition determinants within the ssrA degradation tag allow modulation of proteolysis. *Proc. Natl. Acad. Sci. USA* **98**, 10584–10589 (2001).

7. Lytvynenko, I., Paternoga, H., Thrun, A., Balke, A., Müller, T.A., Chiang, C.H., Nagler, K., Tsaprailis, G., Anders, S., Bischofs, I., Maupin-Furlow, J.A., Spahn, C.M.T. & Joazeiro, C.A.P. (2019) Alanine tails signal proteolysis in bacterial ribosome-associated quality control. *Cell* **178**, 76–90.

8. Siddiqui, S.M., Sauer, R.T. & Baker, T.A. Role of the processing pore of the ClpX AAA+ ATPase in the recognition and engagement of specific protein substrates. *Genes Dev*. **18**, 369–374 (2004).

9. Farrell, C.M., Baker, T.A. & Sauer, R.T. Altered specificity of a AAA+ protease. *Mol. Cell* **25**, 161–166 (2007).

10. Martin, A., Baker, T.A. & Sauer, R.T. Diverse pore loops of the AAA+ ClpX machine mediate unassisted and adaptor-dependent recognition of ssrA-tagged substrates. *Mol. Cell* **29**, 441–450 (2008).

11. Iosefson, O., Nager, A.R., Baker, T.A. & Sauer, R.T. Coordinated gripping of substrate by subunits of a AAA+ proteolytic machine. *Nat. Chem. Biol*. **11**, 201–206 (2015).

12. Olivares, A.O., Baker, T.A. and Sauer, R.T. Mechanical protein unfolding and degradation. *Annu. Rev. Physiol*. **80**, 413–429 (2018).

13. Martin, A., Baker, T.A. & Sauer, R.T. Rebuilt AAA+ motors reveal operating principles for ATP-fuelled machines. *Nature* **437**, 1115–1120 (2005).

14. Fei, X., Bell, T.A., Jenni, S. Stinson, B.M., Baker, T.A., Harrison, S.C., and Sauer, R.T. Structures of the ATP-fueled ClpXP proteolytic machine bound to protein substrate. *eLife* **9**, e52774 (2020).

15. Ripstein, Z.A., Vahidi, S., Houry, W.A., Rubinstein, J.L., and Kay, L.E. A processive rotary mechanism couples substrate unfolding and proteolysis in the ClpXP degradation machinery. *eLife*. **9**, e52158 (2020).

16. Puchades, C., Sandate, C.R., and Lander, G.C. The molecular principles governing the activity and functional diversity of AAA+ proteins. *Nat. Rev. Mol. Cell. Biol*. **21**, 43–58 (2020).

17. Barkow, S.R., Levchenko, I., Baker, T.A., and Sauer, R.T. (2009). Polypeptide translocation by the AAA+ ClpXP protease machine. *Chem. Biol*. **16**, 605–612.

18. Kim, Y.I., Burton, R.E., Burton, B.M., Sauer, R.T., and Baker, T.A. (2000). Dynamics of substrate denaturation and translocation by the ClpXP degradation machine. *Mol. Cell* **5**, 639–648.

19. Nager, A.R., Baker, T.A., and Sauer, R.T. (2011). Stepwise unfolding of a β barrel protein by the AAA+ ClpXP protease. *J. Mol. Biol*. **413**, 4–16.

20. Aubin-Tam, M.E., Olivares, A.O., Sauer, R.T., Baker, T.A. & Lang, M.J. Single-molecule protein unfolding and translocation by an ATP-fueled proteolytic machine. *Cell* **145**, 257–267 (2011).

21. Maillard, R.A., Chistol, G., Sen, G., Righini, M., Tan, J., Kaiser, C.M., Hodges, C., Martin, A. & Bustamante, C. ClpX(P) generates mechanical force to unfold and translocate its protein substrates. *Cell* **45**, 459–469 (2011).

22. Saunders, R.A., Stinson, B.M., Baker, T.A, & Sauer, R.T. Multistep substrate binding and engagement by the AAA+ ClpXP protease. *BioRχiv* https://doi.org/10.1101/2020.05.04.076331.

23. Bell, T.A., Baker. T.A. & Sauer, R.T. Interactions between a subset of substrate side chains and AAA+ motor pore loops determine grip during protein unfolding. *eLife* **8**, e46808 (2019).

24. Ormö, M., Cubitt, A.B., Kallio, K., Gross, L.A., Tsien, R.Y. & Remington, S.J. Crystal structure of the *Aequorea victoria* green fluorescent protein. *Science* **273**, 1392–1395 (1996).

Online Methods

Proteins and Peptides. His_6-tagged variants of *E. coli* ClpX, $ClpX^{\Delta N}$ (residues 62-424), single-chain $ClpX^{\Delta N}$ (units connected by six-residue linkers), full-length ClpX, and ClpP were purified as described[18,25]. Peptide substrates were synthesized as described[17], and mutant variants of $ClpX^{\Delta N}$ or GFP were constructed by PCR as described[25].

Cryo-EM. We combined single-chain $ClpX^{\Delta N}$ (4 μM), ClpP (1.8 μM), and ATPγS (2.5 mM) in buffer containing 20 mM HEPES (pH 7.5), 100 mM KCl, and 25 mM $MgCl_2$. After 5 min at 25 °C, we added an equal volume of GFP-G_3YG_9SENYALAA (20 μM) and ATP (2.5 mM) in the same buffer, and applied 3 μL to glow discharged EM grids (Quantifoil R2/2 400 mesh). The GFP portion of this substrate consisted of residues 1-229. An ATPγS/ATP mixture was used to allow rapid substrate binding, while slowing translocation and unfolding[22]. Samples were blotted and vitrified within 15 s of final mixing. 4525 micrographs were collected using a Talos Arctica with a Gatan K3 direct electron detector (super-resolution pixel 0.435 Å; uncalibrated magnification X45000). EM images contained complexes in which $ClpP_{14}$ was bound to one (~60%) or two (~40%) $ClpX^{\Delta N}$ hexamers. After three rounds of 2D classification, 344,069 complexes with one $ClpX^{\Delta N}$ hexamer were selected for 3D reconstruction. Using a 40-Å low-pass filtered ClpP map as the search model (EMDB: EMD-20434, ref. 14) but no mask, 3D auto-refinement without symmetry (C1) yielded a ClpXP map at 3.5-Å resolution. CTF-refinement and particle polishing improved the overall resolution of this map to 2.8 Å. After focused classification on ClpX without alignment, multiple runs with different class numbers converged to two major classes, which were later named the recognition complex (3.1 Å resolution) and intermediate complex (3.2 Å resolution). Data analysis

and reconstruction was performed within the Relion 3.0.8 pipeline[26]. We docked structures of ClpP (pdb 6PPE) or ClpXP-substrate complexes (pdb 6PP5 and 6PP7) into EM maps using Chimera[27], rigid-body refined ClpX domains using Coot[28], and performed real-space refinement using PHENIX[29]. The ssrA degron was first modeled and refined as polyalanine, and specific side chains were modeled and refined subsequently.

Degradation assays. Peptide degradation by ClpXP (0.3 μM full-length $ClpX_6$; 0.8 μM $ClpP_{14}$) was assayed by changes in fluorescence (excitation/emission: 320/420 nm) at 30 °C in 25 mM HEPES [pH 7.6], 200 mM KCl, 5 mM $MgCl_2$, 0.032% NP-40, 10% glycerol with 4 mM ATP, 16 mM creatine phosphate, and 0.32 mg/ml creatine phosphokinase[17]. Degradation of ssrA-tagged GFP substrates by wild-type or variant $ClpX^{\Delta N}$ hexamers (0.1-0.3 μM) and $ClpP_{14}$ (0.3-0.9 μM) was assayed by changes in fluorescence (excitation/emission: 467/511 nm for low substrate concentrations or 420/540 nm for high substrate concentrations) under similar conditions but at 37 °C, without NP-40, and with 5 mM ATP[18].

To model GFP-YALAA binding to ClpXP, we extended the C-terminal β-strand of GFP (pdb 1EMA; residues 2-229) with the sequence YALAA and aligned this sequence with the YALAA of recognition-complex degron using the PyMOL Molecular Graphics System, v. 2.0 (Schrödinger, LLC). Analysis in MolProbity[30] revealed multiple clashes between GFP and the RKH loops of ClpX, which were minimized manually in Coot[28] by rotation of the residue 2-229 segment of GFP relative to the rest of the complex. To minimize clashes further, we created a map of the modeled complex and optimized

geometry using the Calculate F(model) and Real-space refinement utilities, respectively in PHENIX[28]. The final model had a MolProbity score of 1.0 (100th percentile) and one minor clash (0.44 Å) between GFP and ClpX.

Methods references

25. Stinson, B.M., Nager, A.R., Glynn, S.E., Schmitz, K.R., Baker, T.A. & Sauer, R.T. Nucleotide binding and conformational switching in the hexameric ring of a AAA+ machine. *Cell* **153**, 628–639 (2013).

26. Zivanov, J., Nakane, T., Forsberg, B.O., Kimanius, D., Hagen, W.J., Lindahl, E., & Scheres, S.H. New tools for automated high-resolution cryo-EM structure determination in RELION-3. *eLife* **7**, e42166 (2018).

27. Pettersen, E.F., Goddard, T.D., Huang, C.C., Couch, G.S., Greenblatt, D.M., Meng, E.C. & Ferrin, T.E. UCSF Chimera--a visualization system for exploratory research and analysis. *J. Comput. Chem*. **25**, 1605–1612 (2004).

28. Emsley, P. & Cowtan, K. Coot: model-building tools for molecular graphics. *Acta Cryst. D* **60**, 2126–2132 (2004).

29. Adams, P.V., Afonine, G., Bunkoczi, V.B., Chen, I.W., Davis, N., Echols, J.J., Headd, L.W., Hung, G.J., Kapral, R.W., Grosse-Kunstleve, A.J., McCoy, N.W., Moriarty, R., Oeffner, R., Read, R.J., Richardson, D.C., Richardson, J.S., Terwilliger, T.C. & Zwart,

P.H. PHENIX: a comprehensive Python-based system for macromolecular structure solution. *Acta Cryst*. D **66**, 213–221 (2010).

30. Williams, C.J., Headd, J.J., Moriarty, N.W., Prisant, M.G., Videau, L.L., Deis, L.N., Verma, V., Keedy, D.A., Hintze, B.J., Chen, V.B., Jain, S., Lewis, S.M., Arendall, W.B. 3rd, Snoeyink, J., Adams, P.D., Lovell, S.C., Richardson, J.S., & Richardson, D.C. MolProbity: More and better reference data for improved all-atom structure validation. *Protein Sci*. **27**, 293–315 (2018).

Name	**ClpP**	**ClpXP-ssrA Recognition complex**	**ClpXP-ssrA Intermediate complex**
PDB ID	6WR2	6WRF	6WSG
EMDB ID	EMD-21875	EMD-21882	EMD-21892
	Data collection/processing		
Microscope	Talos Arctica		
Camera	K3		
Magnification	45000X		
Voltage (kV)	200		
Total electron dose ($e^-/Å^2$)	53		
Defocus range (μm)	-1.2 to -2.5		
Pixel size (Å)	0.435		
Micrographs collected	4525		
Final particles	344069	139817	130240
Symmetry	C1	C1	C1
Resolution Å (FSC 0.143)	2.8	3.1	3.2
	Model composition		
Non-hydrogen atoms	21310	26835	25932
Protein residues	2729	3450	3334
Ligands	0	6	5
	Refinement		
Map-model CC	0.82	0.77	0.74
RMSD bond lengths (Å)	0.015	0.003	0.011
RMSD bond angles (degrees)	1.16	0.73	1.13
	Validation		
MolProbity score	0.89	0.94	0.96
Clash score	1.5	1.9	1.7
C-beta deviations	0	0	0
Rotamer outliers (%)	0	0.07	0
Ramachandran favored (%)	98.9	99	99.3
Ramachandran disallowed (%)	0	0	0

Table 1. Cryo-EM data collection, processing, model building, and validation statistics.